Electronic Supplementary Material (ESI) for Soft Matter.

Electronic Supplementary Information

A simple predictor of interface orientation of fluids of disk-like anisotropic particles and its implications for organic semiconductors

Belinda J. Boehm and David M. Huang

Contents

S1 Simulation parameters for organic-semiconductor-like oblate ellipsoids

All simulations used the LAMMPS[1] implementation of the Gay–Berne (GB) potential,[2] which is a generalisation of the original uniaxial GB potential[3] to dissimilar biaxial ellipsoidal particles.[4] In this potential, the anisotropy of the shape of a particle i is defined in terms of the particle's principal diameters, σ_{ai}, σ_{bi}, and σ_{ci}, by the diagonal shape matrix, $\boldsymbol{S}_i = \mathrm{diag}(\sigma_{ai},\sigma_{bi},\sigma_{ci})/2$, while the anisotropy of its interactions is defined in terms of the relative well depths, ϵ_{ai}, ϵ_{bi}, and ϵ_{ci}, along the corresponding axes by the diagonal interaction matrix, $\boldsymbol{E}_i = \mathrm{diag}(\epsilon_{ai},\epsilon_{bi},\epsilon_{ci})$. For the uniaxial oblate ellipsoidal particles studied in this work, $\sigma_{ai} = \sigma_{ci} \equiv \sigma_S$, $\sigma_{bi} \equiv \sigma_F$, $\epsilon_{ai} = \epsilon_{ci} \equiv \epsilon_S$, and $\epsilon_{bi} \equiv \epsilon_F$, where the subscripts "S" and "F" indicate diameters or well depths in the side–side and face–face directions, respectively.

The interaction potential between two particles, i and j, is

$$u_{\mathrm{GB}}\left(\boldsymbol{r}_{ij},\boldsymbol{A}_i,\boldsymbol{A}_j\right) = u_{\mathrm{r}}\left(\boldsymbol{r}_{ij},\boldsymbol{A}_i,\boldsymbol{A}_j\right)\eta\left(\boldsymbol{A}_i,\boldsymbol{A}_j\right)\chi\left(\boldsymbol{r}_{ij},\boldsymbol{A}_i,\boldsymbol{A}_j\right), \tag{S1}$$

where $\boldsymbol{r}_{ij} = \boldsymbol{r}_i - \boldsymbol{r}_j$ is the vector between the particle centres at positions $\boldsymbol{r}_i$ and $\boldsymbol{r}_j$, respectively, and $\boldsymbol{A}_i$ and $\boldsymbol{A}_j$ are rotation matrices transforming the orientations of the two particles from the lab frame to the body frame. The first factor, u_{r}, in eqn (S1) controls the distance dependence of the interaction and takes the form of a shifted Lennard-Jones (LJ) potential,

$$u_{\mathrm{r}}\left(\boldsymbol{r}_{ij},\boldsymbol{A}_i,\boldsymbol{A}_j\right) = 4\epsilon\left[\left(\frac{\sigma}{h_{ij}+\sigma}\right)^{12} - \left(\frac{\sigma}{h_{ij}+\sigma}\right)^{6}\right], \tag{S2}$$

where σ and ϵ define the length and energy scales of the potential, respectively, and h_{ij} is the distance of closest approach of the particles, approximated as[5]

$$h_{ij}\left(\boldsymbol{r}_{ij},\boldsymbol{A}_i,\boldsymbol{A}_j\right) = r_{ij} - \left(\frac{1}{2}\hat{\boldsymbol{r}}_{ij}^{\mathrm{T}}\boldsymbol{G}_{ij}^{-1}\hat{\boldsymbol{r}}_{ij}\right)^{-1/2}, \tag{S3}$$

where $r_{ij} = \left|\boldsymbol{r}_{ij}\right|$, $\hat{\boldsymbol{r}}_{ij} = \boldsymbol{r}_{ij}/r_{ij}$, and

$$\boldsymbol{G}_{ij} = \boldsymbol{A}_i^{\mathrm{T}}\boldsymbol{S}_i^2\boldsymbol{A}_i + \boldsymbol{A}_j^{\mathrm{T}}\boldsymbol{S}_j^2\boldsymbol{A}_j. \tag{S4}$$

The other two factors, η and χ, in eqn (S1) control the position and orientation dependence of the interaction strength, and are given by

$$\eta\left(\boldsymbol{A}_i,\boldsymbol{A}_j\right) = \left[\frac{2\bar{\sigma}_i\bar{\sigma}_j}{\det\left(\boldsymbol{G}_{ij}\right)}\right]^{\nu/2} \tag{S5}$$

and

$$\chi\left(\boldsymbol{r}_{ij},\boldsymbol{A}_i,\boldsymbol{A}_j\right) = \left(2\hat{\boldsymbol{r}}_{ij}^{\mathrm{T}}\boldsymbol{B}_{ij}^{-1}\hat{\boldsymbol{r}}_{ij}\right)^{\mu}, \tag{S6}$$

where

$$\bar{\sigma}_i = \left(\sigma_{ai}\sigma_{bi} + \sigma_{ci}^2\right)\left(\sigma_{ai}\sigma_{bi}\right)^{1/2}, \tag{S7}$$

$$\boldsymbol{B}_{ij} = \boldsymbol{A}_i^{\mathrm{T}}\boldsymbol{E}_i^{-1/\mu}\boldsymbol{A}_i + \boldsymbol{A}_j^{\mathrm{T}}\boldsymbol{E}_j^{-1/\mu}\boldsymbol{A}_j, \tag{S8}$$

and ν and μ are parameters that tune the shape of the potential.

The anisotropy of the GB potential for uniaxial particles can be fully described in terms of two parameters: the shape anisotropy parameter $\kappa = \sigma_F/\sigma_S$ and the interaction anisotropy parameter $\kappa' = \epsilon_S/\epsilon_F$. Parameters used to simulate a range of values of κ and κ' typical of common organic semiconductors (OSCs) are given in Tables S1 and S2, respectively. The parameter range studied is reasonably representative of OSC systems for an energy scale of $\epsilon = 1$ kcal/mol and length scale of $\sigma = 3.2$ Å (bulk density approx 1.1 g cm^{-3} at 560 K and 1 atm for $\kappa = 0.36$, $\kappa' = 0.19$, which is representative of perylene). For all simulations the values of ν and μ previously used to model typical OSCs with the biaxial GB potential were used ($\nu = 1$ and $\mu = 2$).[4]

Particle masses were chosen to maintain the same mass density of a single particle with volume $\frac{\pi\sigma_S^2\sigma_F}{6}$ as the previously published biaxial GB perylene model with volume $\frac{\pi\sigma_S\sigma_F\sigma_E}{6}$ and mass 252.3 g mol^{-1}, where the additional diameter ($i = \mathrm{E}$) corresponds to the third unique principal diameter unique of the biaxial particle (end–end). Table S3 shows the variation of this density for the various published biaxial molecules,[4] and shows that, although there is some variability in this parameter across different molecules, for this wide variety of molecules it is relatively constant at between 1.4 and 1.7 g mol^{-1} Å^{-3}.

OPLS-AA LJ parameters for aromatic carbon[6] or silicon[7] were used to model the solid substrate, with particles placed in the typical arrangements for these surfaces. Substrate particles were treated with the GB potential,

with the elements of the shape matrix and interaction matrix all set to the same value ($\sigma_{ai} = \sigma_{bi} = \sigma_{ci} = \sigma_{\mathrm{LJ}}$, $\epsilon_{ai} = \epsilon_{bi} = \epsilon_{ci} = \epsilon_{\mathrm{LJ}}/\epsilon$). Fluid–substrate interactions were then calculated using the mixing rules defined by eqns (S3)–(S8). For substrate–fluid interactions, σ in eqn S2 was replaced by $(\sigma + \sigma_{\mathrm{LJ}})/2$. Substrate parameters are summarised in Table S4.

Table S1 Shape anisotropy parameter $\kappa = \sigma_{\mathrm{F}}/\sigma_{\mathrm{S}}$ given values of the principal diameter in the face–face (σ_{F}) and side–side (σ_{S}) directions used in the simulations. The size z_{w} of the box in the z-dimension required to constrain the overall volume fraction to the target value of ϕ_{av} is also given.

κ	$\sigma_{\mathrm{F}}/\sigma$	$\sigma_{\mathrm{S}}/\sigma$	ϕ_{av}	z_{w}/σ
0.30	1.03	3.43	0.28	115.63
			0.39	84.06
			0.49	65.94
0.35	1.03	2.94	0.28	85.00
			0.39	61.88
			0.49	48.44
0.40	1.03	2.56	0.28	65.00
			0.39	47.19
			0.49	37.19
0.45	1.03	2.29	0.28	51.25
			0.39	37.50
			0.49	29.38
0.50	1.03	2.06	0.28	41.56
			0.39	30.31
			0.49	23.80

Table S2 Interaction anisotropy parameter $\kappa = \epsilon_{\mathrm{S}}/\epsilon_{\mathrm{F}}$ given values of the well depth in the face–face (ϵ_{F}) and side–side (ϵ_{S}) orientations.

κ'	ϵ_{F}	ϵ_{S}
0.15	6.67	1
0.20	5.00	1
0.25	4.00	1
0.30	3.33	1
0.50	2.00	1
0.70	1.43	1
1.20	1.67	2

Table S3 Mass density of various oblate ellipsoidal molecules, given their molecular weight (MW) and principal diameters σ_i from published biaxial GB models.[4]

compound	MW (g/mol)	σ_{S}	σ_{F}	σ_{E}	density (g/mol/Å^3)
porphine	310.35	11.4	3.2	11.4	1.41
benzene	78.11	6.3	3.1	6.5	1.17
perylene	252.30	8.2	3.3	10.4	1.69
pyrene	202.25	8.1	3.2	10.5	1.40
benzoquinone	108.10	6.0	3.2	7.4	1.44
naphthalene	128.17	6.5	3.3	8.2	1.37
anthraquinone	208.00	7.2	3.2	10.5	1.58
tetrazine	82.06	5.3	3.9	6.9	1.14

Table S4 LJ parameters for substrate particles from the OPLS-AA force field. Particles were treated as GB particles with $\sigma_{ai} = \sigma_{bi} = \sigma_{ci} = \sigma_{\mathrm{LJ}}$, and $\epsilon_{ai} = \epsilon_{bi} = \epsilon_{ci} = \epsilon_{\mathrm{LJ}}/\epsilon$. The substrate labelled "strong" is an artifically strongly interacting substrate with the same structure as graphene and twice the value of ϵ_{LJ}.

	$\epsilon_{\mathrm{sub}}/\epsilon$	$\sigma_{\mathrm{sub}}/\sigma$	$\epsilon_{\mathrm{LJ}}/\epsilon$	$\sigma_{\mathrm{LJ}}/\sigma$
graphene	1	1.11	0.04	1.11
silicon	1	1.25	0.06	1.25
"strong"	1	1.11	0.08	1.11

S2 List of simulated systems

The tables below list all the systems simulated in this work, as well as their key results. Table S5 lists the purely repulsive systems, and Table S6 the systems with both attractive and repulsive interactions. In both cases, a number of systems were not isotropic in the bulk and were not included in the plots in the main text. Due to the lower mobility of the particles in these anisotropic-bulk systems, simulation configurations in these systems were not necessarily sampled from the equilibrium distribution for the molecular dynamics (MD) simulation protocol used in this work.

S2.1 Purely repulsive systems

Table S5 Complete list of the *purely repulsive* systems studied in this work. Items highlighted in red were anisotropic in the bulk and are not included in the plots in the main text. $T^* = k_B T/\epsilon$ is the reduced temperature, ϕ_{av} is the overall volume fraction to which the system was constrained by the position of the harmonic wall (i.e. the average fluid volume fraction between $z = \sigma_{sub}/2$, the surface of the solid substrate, and z_w, the position of the harmonic wall), and ϕ is the volume fraction of particles in the bulk fluid (calculated based on the number of GB particles with centers-of-mass within $\pm 3\sigma_S$ of the center of the system). The orientational order parameter at the solid (s_{sub}) and vapour (s_{vap}) interfaces, and the corresponding orientations (F = face-on, S = side-on) are given in the final four columns. The systems that gave the much less common side-on orientation at the solid substrate are highlighted in bold.

substrate type	T^*	κ	κ'	ϕ_{av}	ϕ	s_{sub}	orient$_{sub}$	s_{vap}	orient$_{vap}$
silicon	0.62	0.30	0.20	0.18	0.19	0.17	F	−0.06	S
silicon	0.62	0.30	0.20	0.28	0.29	0.37	F	−0.26	S
silicon	0.62	0.30	0.20	0.39	0.39	0.71	F	−0.42	S
silicon	0.62	0.30	0.20	0.46	0.46	−0.45	**S**	−0.46	S
silicon	0.62	0.35	0.20	0.18	0.18	0.13	F	−0.06	S
silicon	0.62	0.35	0.20	0.28	0.29	0.23	F	−0.21	S
silicon	0.62	0.35	0.20	0.39	0.39	0.61	F	−0.39	S
silicon	0.62	0.35	0.20	0.46	0.47	0.81	F	−0.45	S
silicon	0.62	0.40	0.20	0.18	0.18	0.10	F	−0.05	S
silicon	0.62	0.40	0.20	0.28	0.29	0.16	F	−0.17	S
silicon	0.62	0.40	0.20	0.39	0.39	0.37	F	−0.35	S
silicon	0.62	0.40	0.20	0.46	0.46	0.65	F	−0.44	S
silicon	0.62	0.45	0.20	0.18	0.18	0.07	F	−0.04	S
silicon	0.62	0.45	0.20	0.28	0.29	0.10	F	−0.14	S
silicon	0.62	0.45	0.20	0.39	0.39	0.19	F	−0.32	S
silicon	0.62	0.45	0.20	0.46	0.46	0.41	F	−0.41	S
silicon	0.62	0.50	0.20	0.18	0.18	0.06	F	−0.04	S
silicon	0.62	0.50	0.20	0.28	0.29	0.07	F	−0.13	S
silicon	0.62	0.50	0.20	0.39	0.39	0.10	F	−0.28	S
silicon	0.62	0.50	0.20	0.46	0.46	0.12	F	−0.38	S
silicon	0.84	0.30	0.20	0.18	0.18	0.15	F	−0.05	S
silicon	0.84	0.30	0.20	0.28	0.29	0.35	F	−0.24	S
silicon	0.84	0.30	0.20	0.39	0.39	0.67	F	−0.40	S
silicon	0.84	0.30	0.20	0.46	0.46	0.63	F	−0.45	S
silicon	0.84	0.35	0.20	0.18	0.18	0.13	F	−0.07	S
silicon	0.84	0.35	0.20	0.28	0.29	0.24	F	−0.20	S
silicon	0.84	0.35	0.20	0.39	0.39	0.56	F	−0.38	S
silicon	0.84	0.35	0.20	0.46	0.46	0.66	F	−0.44	S

Continued on next page

substrate type	T^*	κ	κ'	ϕ_{av}	ϕ	s_{sub}	orient$_{sub}$	s_{vap}	orient$_{vap}$
silicon	0.84	0.40	0.20	0.18	0.18	0.09	F	−0.06	S
silicon	0.84	0.40	0.20	0.28	0.29	0.15	F	−0.16	S
silicon	0.84	0.40	0.20	0.39	0.39	0.33	F	−0.34	S
silicon	0.84	0.40	0.20	0.46	0.46	0.64	F	−0.42	S
silicon	0.84	0.45	0.20	0.18	0.18	0.07	F	−0.05	S
silicon	0.84	0.45	0.20	0.28	0.29	0.11	F	−0.13	S
silicon	0.84	0.45	0.20	0.39	0.39	0.19	F	−0.30	S
silicon	0.84	0.45	0.20	0.46	0.46	0.36	F	−0.39	S
silicon	0.84	0.50	0.20	0.18	0.18	0.05	F	−0.04	S
silicon	0.84	0.50	0.20	0.28	0.29	0.07	F	−0.12	S
silicon	0.84	0.50	0.20	0.39	0.39	0.11	F	−0.27	S
silicon	0.84	0.50	0.20	0.46	0.46	0.16	F	−0.36	S
graphene	0.62	0.30	0.20	0.18	0.18	0.18	F	−0.09	S
graphene	0.62	0.30	0.20	0.28	0.28	0.40	F	−0.25	S
graphene	0.62	0.30	0.20	0.32	0.32	0.51	F	−0.32	S
graphene	0.62	0.30	0.20	0.35	0.35	0.67	F	−0.37	S
graphene	0.62	0.30	0.20	0.39	0.39	0.75	F	−0.41	S
graphene	0.62	0.30	0.20	0.42	0.42	0.83	F	−0.43	S
graphene	0.62	0.30	0.20	0.46	0.45	0.75	F	−0.45	S
graphene	0.62	0.30	0.20	0.49	0.50	0.12	F	−0.47	S
graphene	0.62	0.35	0.20	0.18	0.18	0.14	F	−0.07	S
graphene	0.62	0.35	0.20	0.28	0.28	0.28	F	−0.20	S
graphene	0.62	0.35	0.20	0.32	0.32	0.36	F	−0.26	S
graphene	0.62	0.35	0.20	0.35	0.35	0.46	F	−0.32	S
graphene	0.62	0.35	0.20	0.39	0.38	0.61	F	−0.38	S
graphene	0.62	0.35	0.20	0.42	0.42	0.73	F	−0.42	S
graphene	0.62	0.35	0.20	0.46	0.46	0.67	F	−0.45	S
graphene	0.62	0.35	0.20	0.49	0.48	−0.40	**S**	−0.46	S
graphene	0.62	0.40	0.20	0.18	0.18	0.12	F	−0.06	S
graphene	0.62	0.40	0.20	0.28	0.28	0.20	F	−0.17	S
graphene	0.62	0.40	0.20	0.32	0.32	0.25	F	−0.22	S
graphene	0.62	0.40	0.20	0.35	0.35	0.32	F	−0.29	S
graphene	0.62	0.40	0.20	0.39	0.38	0.41	F	−0.34	S
graphene	0.62	0.40	0.20	0.42	0.42	0.56	F	−0.39	S
graphene	0.62	0.40	0.20	0.46	0.45	0.69	F	−0.43	S
graphene	0.62	0.40	0.20	0.49	0.49	−0.37	**S**	−0.45	S
graphene	0.62	0.45	0.20	0.18	0.18	0.09	F	−0.05	S
graphene	0.62	0.45	0.20	0.28	0.28	0.15	F	−0.14	S
graphene	0.62	0.45	0.20	0.32	0.32	0.18	F	−0.19	S
graphene	0.62	0.45	0.20	0.35	0.35	0.22	F	−0.25	S
graphene	0.62	0.45	0.20	0.39	0.39	0.29	F	−0.31	S
graphene	0.62	0.45	0.20	0.42	0.42	0.37	F	−0.36	S
graphene	0.62	0.45	0.20	0.46	0.45	0.51	F	−0.40	S
graphene	0.62	0.45	0.20	0.49	0.47	0.67	F	−0.45	S
graphene	0.62	0.50	0.20	0.18	0.18	0.07	F	−0.04	S

Continued on next page

substrate type	T^*	κ	κ'	ϕ_{av}	ϕ	s_{sub}	orient$_{sub}$	s_{vap}	orient$_{vap}$
graphene	0.62	0.50	0.20	0.28	0.28	0.10	F	−0.12	S
graphene	0.62	0.50	0.20	0.32	0.32	0.12	F	−0.17	S
graphene	0.62	0.50	0.20	0.35	0.35	0.15	F	−0.22	S
graphene	0.62	0.50	0.20	0.39	0.39	0.19	F	−0.26	S
graphene	0.62	0.50	0.20	0.42	0.42	0.25	F	−0.32	S
graphene	0.62	0.50	0.20	0.46	0.45	0.33	F	−0.37	S
graphene	0.62	0.50	0.20	0.49	0.49	0.49	F	−0.42	S

S2.2 Attractive–repulsive systems

Table S6 Complete list of the *attractive* systems studied in this work. Items highlighted in red were anisotropic in the bulk and are not included in the plots in the main text. $T^* = k_B T/\epsilon$ is the reduced temperature, ϕ_{av} is the overall volume fraction to which the system was constrained by the position of the harmonic wall (i.e. the average fluid volume fraction between $z = \sigma_{sub}/2$, the surface of the solid substrate, and z_w, the position of the harmonic wall), and ϕ is the volume fraction of particles in the bulk fluid (calculated based on the number of GB particles with centers-of-mass within $\pm 3\sigma_S$ of the center of the system). $P^* = P/(\epsilon/\sigma^3)$ is the reduced pressure, measured as the normal force per unit area acting on the solid substrate. The orientational order parameter at the solid (s_{sub}) and vapour (s_{vap}) interfaces, and the corresponding orientations (F = face-on, S = side-on) are given in the final four columns. The systems that gave the much less common side-on orientation at the solid substrate are highlighted in bold.

substrate type	T^*	κ	κ'	ϕ_{av}	ϕ	P^*	s_{sub}	orient$_{sub}$	s_{vap}	orient$_{vap}$
graphene	0.56	0.40	0.15	0.39	0.53	−3.18	0.07	F	−0.29	S
graphene	0.56	0.40	0.20	0.39	0.53	−9.35	0.32	F	−0.00	S
graphene	0.56	0.40	0.25	0.39	0.44	0.65	0.16	F	−0.00	S
graphene	0.56	0.40	0.30	0.39	0.43	−0.63	0.20	F	0.00	F
graphene	0.56	0.40	0.50	0.39	0.40	51.30	0.28	F	0.01	F
graphene	0.56	0.40	0.70	0.39	0.39	100.99	0.34	F	0.00	F
graphene	**0.56**	**0.45**	**0.15**	**0.39**	**0.53**	**2.40**	**−0.30**	**S**	**−0.13**	**S**
graphene	**0.56**	**0.45**	**0.20**	**0.39**	**0.54**	**4.54**	**−0.44**	**S**	**−0.42**	**S**
graphene	0.56	0.45	0.25	0.39	0.46	−3.85	0.10	F	−0.01	S
graphene	0.56	0.45	0.30	0.39	0.45	2.01	0.14	F	0.01	F
graphene	0.56	0.45	0.50	0.39	0.41	16.24	0.20	F	0.02	F
graphene	0.56	0.45	0.70	0.39	0.40	61.66	0.24	F	0.02	F
graphene	0.56	0.50	0.15	0.39	0.54	−3.42	0.03	F	0.41	F
graphene	**0.56**	**0.50**	**0.20**	**0.39**	**0.56**	**−1.56**	**−0.45**	**S**	**−0.42**	**S**
graphene	0.56	0.50	0.25	0.39	0.48	−1.29	0.03	F	−0.03	S
graphene	0.56	0.50	0.30	0.39	0.47	−5.46	0.08	F	−0.00	S
graphene	0.56	0.50	0.50	0.39	0.43	−2.25	0.15	F	0.02	F
graphene	0.56	0.50	0.70	0.39	0.41	31.89	0.18	F	0.02	F
graphene	**0.62**	**0.30**	**0.15**	**0.39**	**0.53**	**3.25**	**−0.31**	**S**	**0.87**	**F**
graphene	0.62	0.30	0.20	0.39	0.55	10.91	0.79	F	−0.14	S
graphene	0.62	0.30	0.25	0.39	0.36	30.77	0.85	F	−0.05	S
graphene	0.62	0.30	0.30	0.39	0.39	99.24	0.47	F	−0.11	S
graphene	**0.62**	**0.35**	**0.15**	**0.39**	**0.51**	**−4.83**	**−0.14**	**S**	**−0.01**	**S**
graphene	0.62	0.35	0.20	0.39	0.42	1.23	0.13	F	−0.01	S
graphene	0.62	0.35	0.25	0.39	0.40	31.20	0.24	F	−0.02	S
graphene	0.62	0.35	0.30	0.39	0.39	63.98	0.28	F	−0.04	S
graphene	0.62	0.40	0.15	0.39	0.53	1.78	0.32	F	0.13	F
graphene	0.62	0.40	0.20	0.39	0.44	−1.95	0.05	F	−0.03	S
graphene	0.62	0.40	0.25	0.39	0.42	9.10	0.13	F	−0.00	S
graphene	0.62	0.40	0.30	0.39	0.41	25.53	0.18	F	0.01	F
graphene	**0.62**	**0.45**	**0.15**	**0.39**	**0.53**	**−9.52**	**−0.46**	**S**	**0.62**	**F**
graphene	0.62	0.45	0.20	0.39	0.46	4.24	0.00	F	−0.04	S
graphene	0.62	0.45	0.25	0.39	0.44	−1.49	0.09	F	−0.01	S
graphene	0.62	0.45	0.30	0.39	0.43	0.83	0.12	F	0.00	F

Continued on next page

substrate type	T^*	κ	κ'	ϕ_{av}	ϕ	P^*	s_{sub}	orient$_{sub}$	s_{vap}	orient$_{vap}$
graphene	0.62	0.50	0.15	0.39	0.55	−3.38	0.60	F	0.56	F
graphene	**0.62**	**0.50**	**0.20**	**0.39**	**0.47**	**−2.95**	**−0.05**	**S**	**−0.05**	**S**
graphene	0.62	0.50	0.25	0.39	0.46	−0.36	0.04	F	−0.01	S
graphene	0.62	0.50	0.30	0.39	0.45	−2.67	0.07	F	−0.00	S
graphene	**0.73**	**0.30**	**0.15**	**0.39**	**0.48**	**6.45**	**−0.25**	**S**	**0.16**	**F**
graphene	0.73	0.30	0.20	0.39	0.37	51.20	0.21	F	−0.09	S
graphene	0.73	0.30	0.25	0.39	0.38	140.89	0.51	F	−0.18	S
graphene	0.73	0.30	0.30	0.39	0.39	160.90	0.45	F	−0.17	S
graphene	0.73	0.30	1.20	0.39	0.51	10.81	0.86	F	0.55	F
graphene	0.73	0.35	0.15	0.39	0.50	1.55	0.03	F	0.28	F
graphene	0.73	0.35	0.20	0.39	0.39	72.54	0.19	F	−0.12	S
graphene	0.73	0.35	0.25	0.39	0.39	120.80	0.28	F	−0.11	S
graphene	0.73	0.35	0.30	0.39	0.39	152.56	0.31	F	−0.11	S
graphene	0.73	0.35	1.20	0.39	0.49	−1.10	0.83	F	0.42	F
graphene	**0.73**	**0.40**	**0.15**	**0.39**	**0.52**	**0.09**	**−0.05**	**S**	**0.40**	**F**
graphene	0.73	0.40	0.20	0.39	0.40	48.12	0.09	F	−0.03	S
graphene	0.73	0.40	0.25	0.39	0.40	85.89	0.16	F	−0.04	S
graphene	0.73	0.40	0.30	0.39	0.39	124.30	0.20	F	−0.05	S
graphene	0.73	0.40	1.20	0.39	0.44	−8.62	0.66	F	0.14	F
graphene	**0.73**	**0.45**	**0.15**	**0.39**	**0.53**	**10.94**	**−0.46**	**S**	**−0.13**	**S**
graphene	0.73	0.45	0.20	0.39	0.42	1.03	0.03	F	−0.02	S
graphene	0.73	0.45	0.25	0.39	0.41	24.60	0.09	F	−0.01	S
graphene	0.73	0.45	0.30	0.39	0.40	66.25	0.12	F	−0.02	S
graphene	0.73	0.45	1.20	0.39	0.45	−0.60	0.46	F	0.12	F
graphene	**0.73**	**0.50**	**0.15**	**0.39**	**0.54**	**−2.20**	**−0.45**	**S**	**−0.34**	**S**
graphene	**0.73**	**0.50**	**0.20**	**0.39**	**0.44**	**0.58**	**−0.01**	**S**	**−0.03**	**S**
graphene	0.73	0.50	0.25	0.39	0.43	6.87	0.04	F	−0.01	S
graphene	0.73	0.50	0.30	0.39	0.41	28.52	0.07	F	−0.00	S
graphene	0.73	0.50	1.20	0.39	0.47	7.47	0.36	F	0.10	F
graphene	0.84	0.30	0.15	0.39	0.49	32.68	0.10	F	−0.00	S
graphene	0.84	0.30	0.20	0.39	0.39	179.11	0.44	F	−0.23	S
graphene	0.84	0.30	0.25	0.39	0.39	222.26	0.47	F	−0.24	S
graphene	0.84	0.30	0.30	0.39	0.39	268.33	0.50	F	−0.23	S
graphene	0.84	0.35	0.15	0.39	0.41	35.60	0.07	F	−0.03	S
graphene	0.84	0.35	0.20	0.39	0.39	186.33	0.25	F	−0.16	S
graphene	0.84	0.35	0.25	0.39	0.39	230.39	0.30	F	−0.15	S
graphene	0.84	0.35	0.30	0.39	0.39	265.63	0.33	F	−0.15	S
graphene	**0.84**	**0.40**	**0.15**	**0.39**	**0.40**	**67.48**	**−0.01**	**S**	**−0.10**	**S**
graphene	0.84	0.40	0.20	0.39	0.40	144.52	0.13	F	−0.09	S
graphene	0.84	0.40	0.25	0.39	0.39	211.95	0.19	F	−0.09	S
graphene	0.84	0.40	0.30	0.39	0.39	244.84	0.22	F	−0.09	S
graphene	**0.84**	**0.45**	**0.15**	**0.39**	**0.41**	**24.87**	**−0.05**	**S**	**−0.05**	**S**
graphene	0.84	0.45	0.20	0.39	0.40	85.53	0.06	F	−0.05	S
graphene	0.84	0.45	0.25	0.39	0.40	145.06	0.11	F	−0.05	S

Continued on next page

substrate type	T^*	κ	κ'	ϕ_{av}	ϕ	P^*	s_{sub}	orient$_{sub}$	s_{vap}	orient$_{vap}$
graphene	0.84	0.45	0.30	0.39	0.39	185.75	0.14	F	−0.06	S
graphene	**0.84**	**0.50**	**0.15**	**0.39**	**0.43**	**5.58**	**−0.09**	**S**	**−0.05**	**S**
graphene	0.84	0.50	0.20	0.39	0.41	54.45	0.01	F	−0.02	S
graphene	0.84	0.50	0.25	0.39	0.41	102.42	0.06	F	−0.03	S
graphene	0.84	0.50	0.30	0.39	0.40	171.51	0.08	F	−0.03	S
silicon	0.56	0.40	0.15	0.39	0.52	0.55	0.13	F	0.00	F
silicon	0.56	0.40	0.20	0.39	0.53	0.49	0.75	F	0.14	F
silicon	0.56	0.40	0.25	0.39	0.44	3.06	0.01	F	−0.01	S
silicon	0.56	0.40	0.30	0.39	0.43	7.25	0.03	F	0.01	F
silicon	0.56	0.40	0.50	0.39	0.41	76.82	0.12	F	0.00	F
silicon	0.56	0.40	0.70	0.39	0.40	135.44	0.19	F	0.00	F
silicon	0.56	0.45	0.15	0.39	0.53	0.20	0.27	F	−0.08	S
silicon	**0.56**	**0.45**	**0.20**	**0.39**	**0.48**	**−0.16**	**−0.08**	**S**	**−0.07**	**S**
silicon	**0.56**	**0.45**	**0.25**	**0.39**	**0.46**	**2.08**	**−0.01**	**S**	**−0.02**	**S**
silicon	0.56	0.45	0.30	0.39	0.45	−0.51	0.02	F	0.00	F
silicon	0.56	0.45	0.50	0.39	0.42	38.87	0.07	F	0.02	F
silicon	0.56	0.45	0.70	0.39	0.41	102.01	0.12	F	0.02	F
silicon	0.56	0.50	0.15	0.39	0.54	0.36	0.53	F	0.14	F
silicon	**0.56**	**0.50**	**0.20**	**0.39**	**0.49**	**−1.56**	**−0.11**	**S**	**−0.08**	**S**
silicon	**0.56**	**0.50**	**0.25**	**0.39**	**0.48**	**−2.59**	**−0.03**	**S**	**−0.03**	**S**
silicon	0.56	0.50	0.30	0.39	0.47	0.54	0.00	F	−0.00	S
silicon	0.56	0.50	0.50	0.39	0.44	16.57	0.04	F	0.02	F
silicon	0.56	0.50	0.70	0.39	0.42	71.13	0.07	F	0.01	F
silicon	0.62	0.30	0.15	0.39	0.51	0.92	0.04	F	0.05	F
silicon	**0.62**	**0.30**	**0.20**	**0.39**	**0.52**	**2.32**	**−0.13**	**S**	**0.34**	**F**
silicon	0.62	0.30	0.25	0.39	0.37	46.17	0.11	F	−0.06	S
silicon	0.62	0.30	0.30	0.39	0.40	105.42	0.36	F	−0.15	S
silicon	0.62	0.35	0.15	0.39	0.51	−0.15	0.13	F	−0.37	S
silicon	0.62	0.35	0.20	0.39	0.55	0.67	0.13	F	0.06	F
silicon	0.62	0.35	0.25	0.39	0.41	48.99	0.06	F	−0.06	S
silicon	0.62	0.35	0.30	0.39	0.40	82.29	0.12	F	−0.07	S
silicon	0.62	0.40	0.15	0.39	0.52	−0.53	0.21	F	0.38	F
silicon	**0.62**	**0.40**	**0.20**	**0.39**	**0.44**	**4.26**	**−0.03**	**S**	**−0.03**	**S**
silicon	0.62	0.40	0.25	0.39	0.42	20.01	0.02	F	−0.01	S
silicon	0.62	0.40	0.30	0.39	0.41	44.82	0.05	F	−0.01	S
silicon	0.62	0.45	0.15	0.39	0.53	1.33	0.33	F	0.12	F
silicon	**0.62**	**0.45**	**0.20**	**0.39**	**0.46**	**−0.60**	**−0.05**	**S**	**−0.04**	**S**
silicon	0.62	0.45	0.25	0.39	0.44	3.46	0.00	F	−0.01	S
silicon	0.62	0.45	0.30	0.39	0.43	14.95	0.02	F	0.01	F
silicon	**0.62**	**0.50**	**0.15**	**0.39**	**0.54**	**0.91**	**−0.13**	**S**	**0.66**	**F**
silicon	**0.62**	**0.50**	**0.20**	**0.39**	**0.47**	**2.32**	**−0.08**	**S**	**−0.06**	**S**
silicon	**0.62**	**0.50**	**0.25**	**0.39**	**0.46**	**1.50**	**−0.02**	**S**	**−0.02**	**S**
silicon	0.62	0.50	0.30	0.39	0.45	5.02	0.01	F	−0.00	S
strong	0.73	0.30	0.15	0.39	0.56	3.96	0.37	F	0.20	F

Continued on next page

substrate type	T^*	κ	κ'	ϕ_{av}	ϕ	P^*	s_{sub}	orient$_{sub}$	s_{vap}	orient$_{vap}$
strong	0.73	0.30	0.20	0.39	0.38	53.85	0.88	F	−0.11	S
strong	0.73	0.30	0.25	0.39	0.38	135.93	0.85	F	−0.19	S
strong	0.73	0.30	0.30	0.39	0.39	175.05	0.53	F	−0.19	S
strong	0.73	0.35	0.15	0.39	0.54	−0.16	0.83	F	0.45	F
strong	0.73	0.35	0.20	0.39	0.39	81.81	0.35	F	−0.11	S
strong	0.73	0.35	0.25	0.39	0.39	114.61	0.38	F	−0.10	S
strong	0.73	0.35	0.30	0.39	0.39	154.31	0.39	F	−0.11	S
strong	0.73	0.40	0.15	0.39	0.51	−2.32	0.55	F	−0.17	S
strong	0.73	0.40	0.20	0.39	0.40	30.86	0.23	F	−0.02	S
strong	0.73	0.40	0.25	0.39	0.40	73.55	0.28	F	−0.04	S
strong	0.73	0.40	0.30	0.39	0.39	112.77	0.31	F	−0.05	S
strong	**0.73**	**0.45**	**0.15**	**0.39**	**0.55**	**−1.31**	**−0.45**	**S**	**−0.43**	**S**
strong	0.73	0.45	0.20	0.39	0.42	5.02	0.15	F	−0.01	S
strong	0.73	0.45	0.25	0.39	0.41	24.41	0.19	F	−0.01	S
strong	0.73	0.45	0.30	0.39	0.40	76.86	0.23	F	−0.01	S
strong	**0.73**	**0.50**	**0.15**	**0.39**	**0.55**	**6.90**	**−0.46**	**S**	**−0.40**	**S**
strong	0.73	0.50	0.20	0.39	0.44	6.84	0.07	F	−0.02	S
strong	0.73	0.50	0.25	0.39	0.43	−1.09	0.13	F	−0.01	S
strong	0.73	0.50	0.30	0.39	0.41	14.99	0.16	F	−0.00	S
graphene	**0.73**	**0.30**	**0.15**	**0.28**	**0.46**	**3.89**	**−0.22**	**S**	**−0.24**	**S**
graphene	0.73	0.30	0.20	0.28	0.31	24.03	0.20	F	−0.00	S
graphene	0.73	0.30	0.25	0.28	0.30	35.74	0.27	F	−0.03	S
graphene	0.73	0.30	0.30	0.28	0.30	51.85	0.30	F	−0.03	S
graphene	**0.73**	**0.35**	**0.15**	**0.28**	**0.43**	**−3.31**	**−0.03**	**S**	**−0.26**	**S**
graphene	0.73	0.35	0.20	0.28	0.33	12.28	0.12	F	−0.00	S
graphene	0.73	0.35	0.25	0.28	0.30	24.35	0.16	F	−0.00	S
graphene	0.73	0.35	0.30	0.28	0.29	27.60	0.20	F	−0.00	S
graphene	0.73	0.40	0.15	0.28	0.42	4.15	0.13	F	−0.10	S
graphene	0.73	0.40	0.20	0.28	0.39	5.24	0.08	F	−0.00	S
graphene	0.73	0.40	0.25	0.28	0.36	4.72	0.11	F	−0.00	S
graphene	0.73	0.40	0.30	0.28	0.32	15.13	0.13	F	0.00	F
graphene	0.73	0.45	0.15	0.28	0.37	−5.80	0.68	F	0.58	F
graphene	0.73	0.45	0.20	0.28	0.42	8.69	0.03	F	−0.01	S
graphene	0.73	0.45	0.25	0.28	0.40	5.97	0.08	F	−0.00	S
graphene	0.73	0.45	0.30	0.28	0.38	11.34	0.09	F	−0.00	S
graphene	**0.73**	**0.50**	**0.15**	**0.28**	**0.39**	**1.48**	**−0.09**	**S**	**0.69**	**F**
graphene	**0.73**	**0.50**	**0.20**	**0.28**	**0.44**	**−0.64**	**−0.01**	**S**	**−0.02**	**S**
graphene	0.73	0.50	0.25	0.28	0.42	3.46	0.04	F	−0.01	S
graphene	0.73	0.50	0.30	0.28	0.41	0.10	0.07	F	0.00	F
graphene	**0.73**	**0.30**	**0.15**	**0.49**	**0.50**	**62.01**	**−0.35**	**S**	**−0.36**	**S**
graphene	**0.73**	**0.30**	**0.20**	**0.49**	**0.51**	**109.18**	**−0.07**	**S**	**−0.36**	**S**
graphene	0.73	0.30	0.25	0.49	0.48	181.89	0.15	F	−0.32	S
graphene	0.73	0.30	0.30	0.49	0.52	263.23	0.48	F	−0.28	S
graphene	**0.73**	**0.35**	**0.15**	**0.49**	**0.52**	**43.38**	**−0.46**	**S**	**−0.25**	**S**

Continued on next page

substrate type	T^*	κ	κ'	ϕ_{av}	ϕ	P^*	s_{sub}	orient$_{sub}$	s_{vap}	orient$_{vap}$
graphene	**0.73**	**0.35**	**0.20**	**0.49**	**0.48**	**151.11**	**−0.42**	**S**	**−0.31**	**S**
graphene	0.73	0.35	0.25	0.49	0.51	350.30	0.36	F	−0.24	S
graphene	0.73	0.35	0.30	0.49	0.53	454.14	0.50	F	−0.27	S
graphene	**0.73**	**0.40**	**0.15**	**0.49**	**0.52**	**30.11**	**−0.19**	**S**	**−0.38**	**S**
graphene	**0.73**	**0.40**	**0.20**	**0.49**	**0.48**	**319.78**	**−0.16**	**S**	**−0.40**	**S**
graphene	0.73	0.40	0.25	0.49	0.47	775.73	0.41	F	−0.40	S
graphene	0.73	0.40	0.30	0.49	0.49	952.70	0.57	F	−0.34	S
graphene	**0.73**	**0.45**	**0.15**	**0.49**	**0.55**	**24.49**	**−0.14**	**S**	**−0.23**	**S**
graphene	0.73	0.45	0.20	0.49	0.49	818.67	0.30	F	−0.34	S
graphene	0.73	0.45	0.25	0.49	0.49	953.54	0.36	F	−0.30	S
graphene	0.73	0.45	0.30	0.49	0.49	1053.37	0.39	F	−0.28	S
graphene	**0.73**	**0.50**	**0.15**	**0.49**	**0.52**	**6.56**	**−0.46**	**S**	**−0.44**	**S**
graphene	0.73	0.50	0.20	0.49	0.50	896.87	0.13	F	−0.30	S
graphene	0.73	0.50	0.25	0.49	0.50	1073.39	0.23	F	−0.27	S
graphene	0.73	0.50	0.30	0.49	0.50	1155.16	0.27	F	−0.25	S

S3 Substrate parameters and effect on alignment

Two different substrates structures were examined to determine the effect of interaction strength and substrate features on alignment at the solid interface. Interaction parameters for the different substrates can be found in section S1 Table S4. The arrangement of particles in the two substrates, shown in Fig. S1, was chosen to mimic that of graphene (atom spacing from the OPLS-AA force field for the equilibrium bond length between aromatic carbons[6]), and the fcc(001) plane of silicon's crystal structure (spacing matching silicon's lattice constant)[8] for $\sigma = 3.2$ Å.

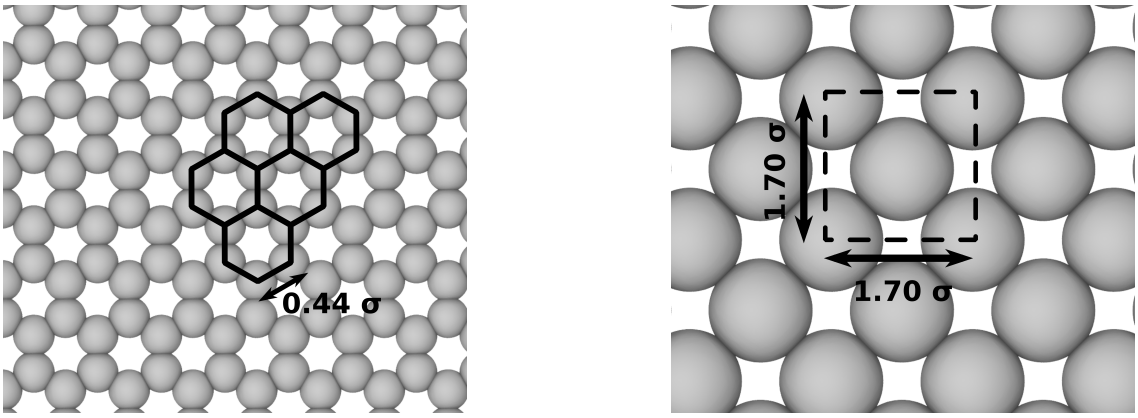

(a) Graphene substrate. Hexagons highlight the positions of the aromatic rings. Distance between all connected carbon atoms is 0.44 σ.

(b) Silicon substrate. Dashed lines indicate the unit cell

Fig. S1 Structures of the atomistic substrates used to model the solid substrate.

The dependence of the orientational ordering at the solid and vapour interfaces on the substrate is shown below. At the solid interface, stronger substrate–fluid interactions push the points further left (towards a more face-on orientation) on the phase diagram. The substrate has a negligible effect on the orientation at the vapour interface, as expected. A slight dependence of the alignment at the solid interface on the substrate structure is observed, with the less densely packed silicon substrate giving a slight shift towards the side-on orientation. This can be explained by considering the non-uniform silicon surface as a surface that is slightly penetrable in certain regions, so excluded volume entropic effects are expected to slightly enhance the side-on orientation relative to the face-on for this substrate.

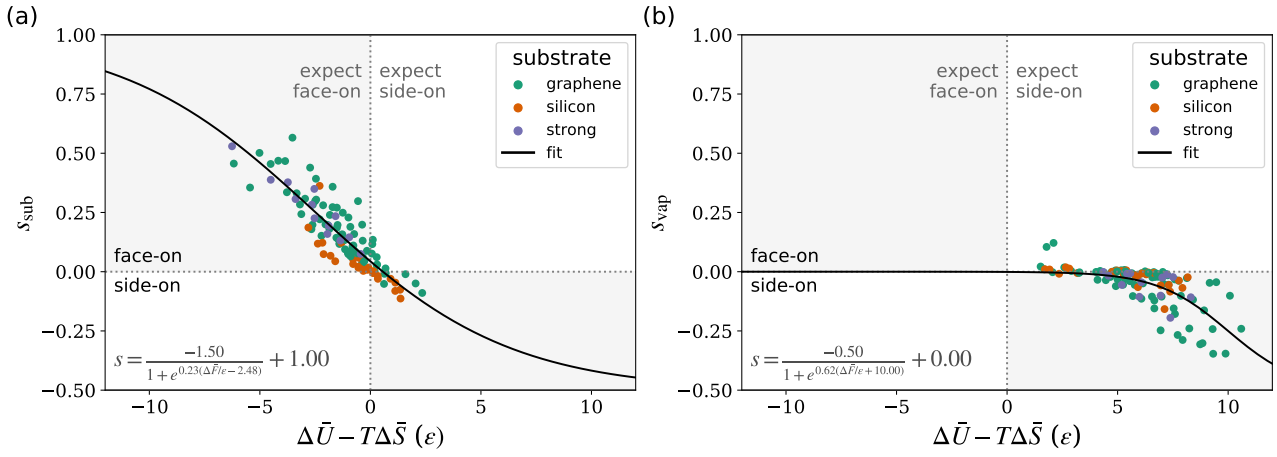

Fig. S2 Orientational order parameter at the (a) substrate and (b) vapour interfaces as a function of interfacial free energy difference for different substrate types.

S4 Dependence of entropy on substrate and temperature

The calculations presented for the entropy difference between the face-on and the side-on alignment at the two interfaces used data from simulations with two different substrates and at different temperatures. The dependence of the entropy scaling on these two factors is shown below (Figs. S3, S4). In all cases, the entropy does not significantly depend on the simulation conditions, though some variability with the substrate structure, as discussed in the main paper, is observed.

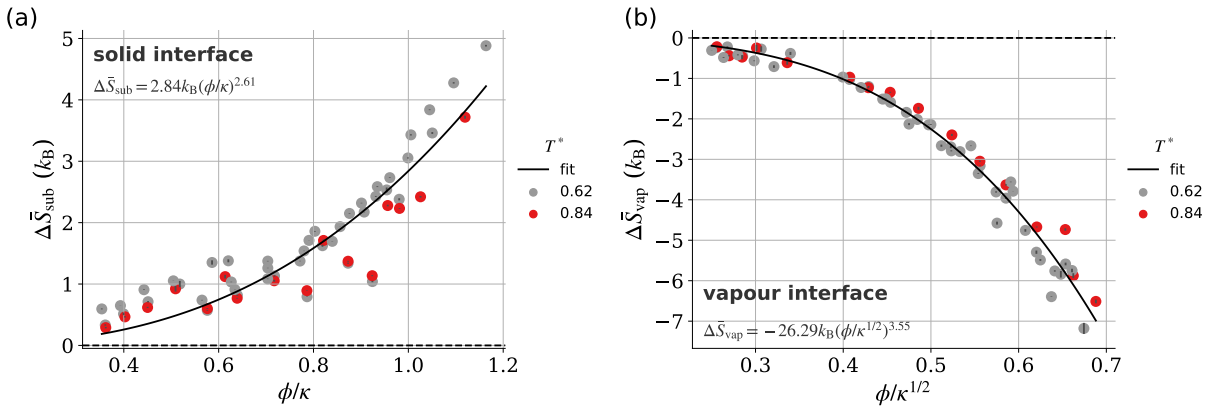

Fig. S3 Entropy difference between face-on and side-on orientations per interface particle at the (a) solid and (b) vapour interfaces for different simulation temperatures.

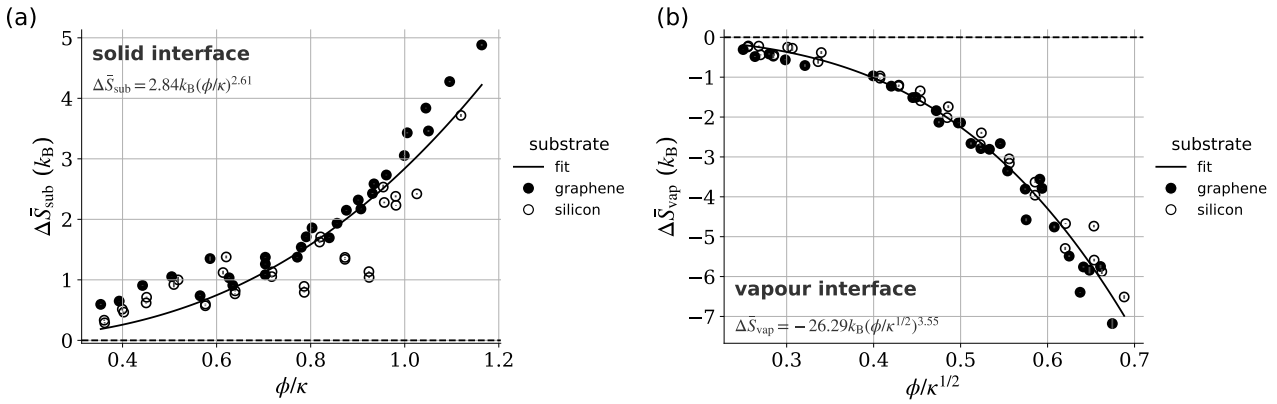

Fig. S4 Entropy difference between face-on and side-on orientations per interface particle at the (a) solid and (b) vapour interfaces for different substrate types.

S5 Selected density/order parameter profiles

The density and orientational order parameter profiles for selected systems is shown. The systems chosen are those that displayed the greatest orientation preference at either interface, and one that is close to isotropic.

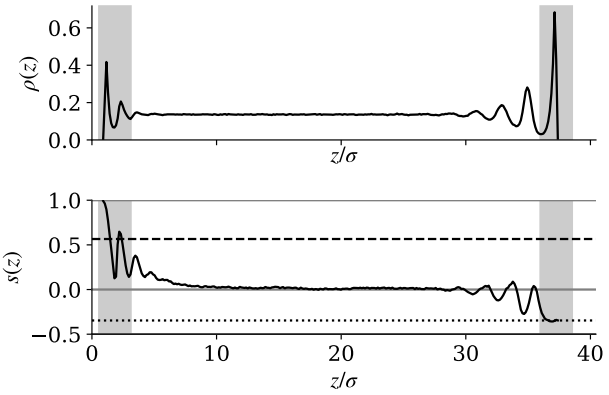

(a) Strongest side-on alignment at vapour interface, and strongest face-on alignment at solid interface: graphene substrate, $\kappa = 0.4$, $\kappa' = 0.3$, $T^* = 0.73$, $\phi_{\text{av}} = 0.49$, $\phi = 0.49$, $P^* = 953$

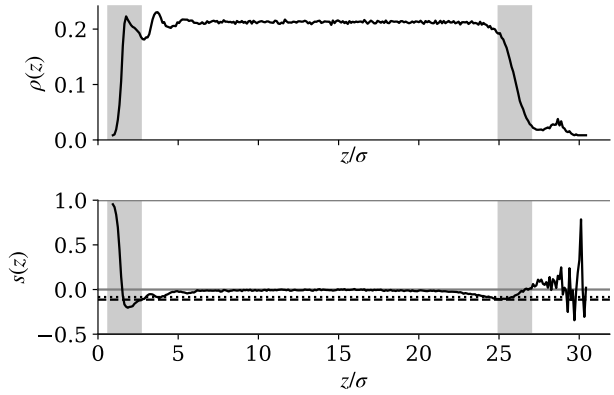

(b) Strongest side-on alignment at solid interface: silicon substrate, $\kappa = 0.5$, $\kappa' = 0.2$, $T^* = 0.56$, $\phi_{\text{av}} = 0.39$, $\phi = 0.49$, $P^* = -1.5$.

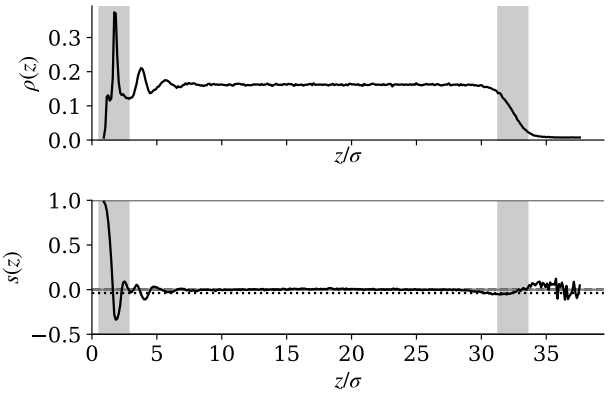

(c) System close to isotropic at both interfaces: graphene substrate $\kappa = 0.45$, $\kappa' = 0.2$, $T^* = 0.62$, $\phi_{\text{av}} = 0.39$, $\phi = 0.46$, $P^* = 4.2$.

Fig. S5 Density ($\rho(z)$, top) and orientational order parameter ($s(z)$, bottom) profiles for a selection of systems showing the most extreme of the possible behaviours at each interface. Shaded regions indicate the z coordinates of particles that were considered to be at the solid or vapour interface when calculating s_{sub} and s_{vap}. In all cases, $s(z) \to 1$ as $z \to 0$ since only particles in the face-on orientation can have their centres-of-mass within that distance of the substrate. Hence, the value of s_{sub} is calculated as the average over all particles within the shaded grey regions. Dotted (s_{vap}) and dashed (s_{sub}) lines indicate these interface values. The particles in the solid substrate are centred at at $z = 0$.

S6 Orientation distributions at solid and vapour interfaces

The orientation distributions at the solid and vapour interfaces for a selection of the systems of purely repulsive particles, used to calculate the entropic component of the free energy, are shown in Fig. S6. All distributions below are for the graphene arrangement of substrate particles at $T^* = 0.62$. θ is the angle between the short of the fluid particle and the z-axis (normal to the substrate). $\cos(\theta) = 0$ corresponds to the perfectly side-on orientation, and $\cos(\theta) = 1$ to perfectly face-on.

Note that conditions for which $P(\cos(\theta) = 1)$ was found to be zero (due to the finite simulation duration and very low probability of these configurations) were not used in the determination of the scaling of the face-on/side-on entropy difference with ϕ and κ. These conditions were found to correspond to systems for which the bulk fluid was not isotropic and so were not used in predicting interface orientation in the paper.

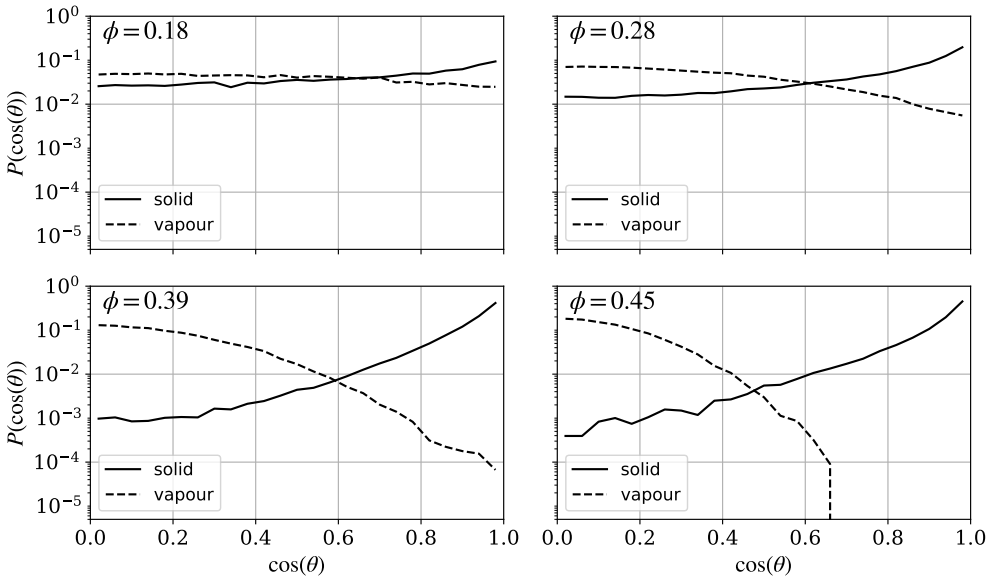

(a) $\kappa = 0.30$

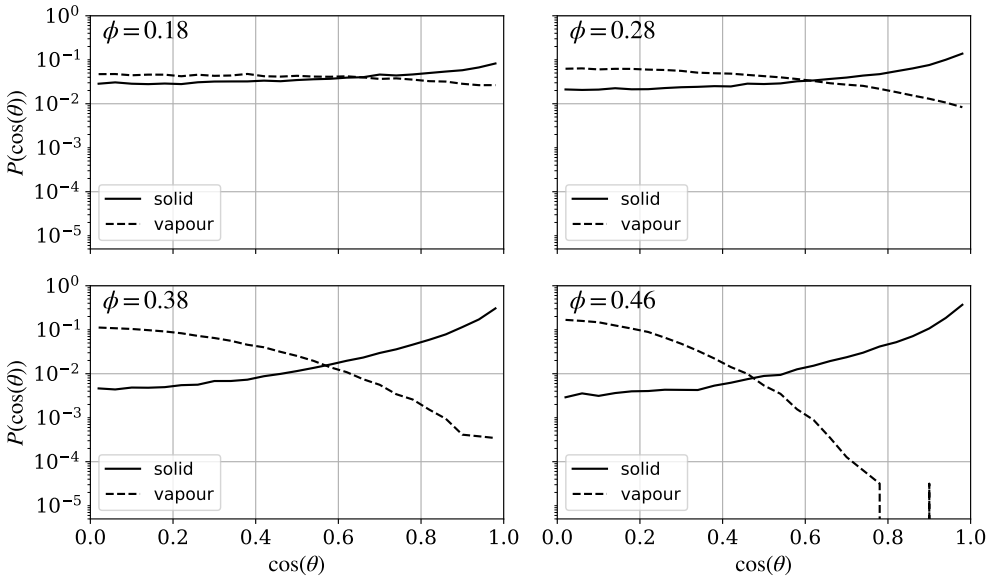

(b) $\kappa = 0.35$

Fig. S6 Orientation distributions at the interfaces in simulations of purely repulsive particles. Solid lines are the distributions at the solid interface and dashed lines are those at the vapour interface.

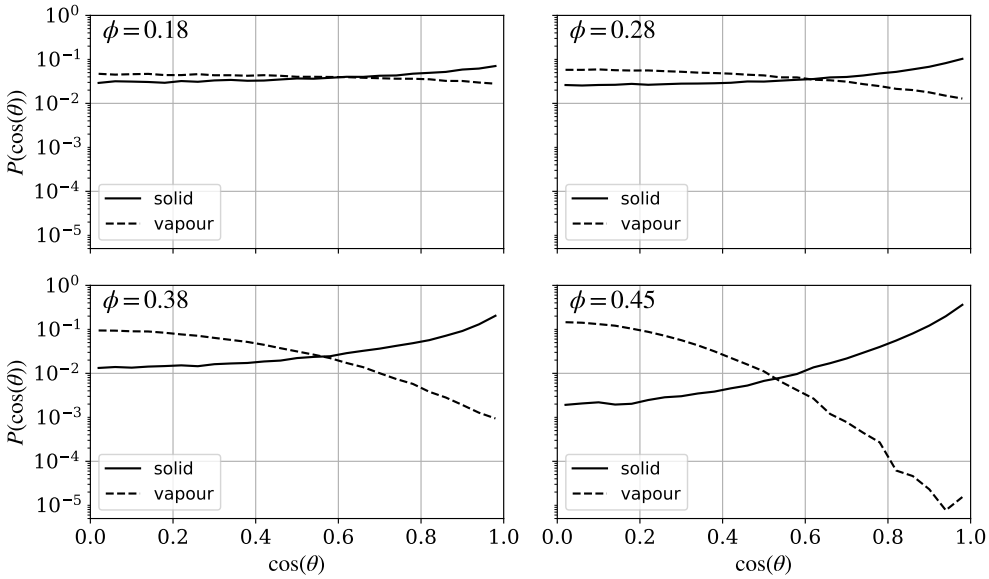

(c) $\kappa = 0.40$

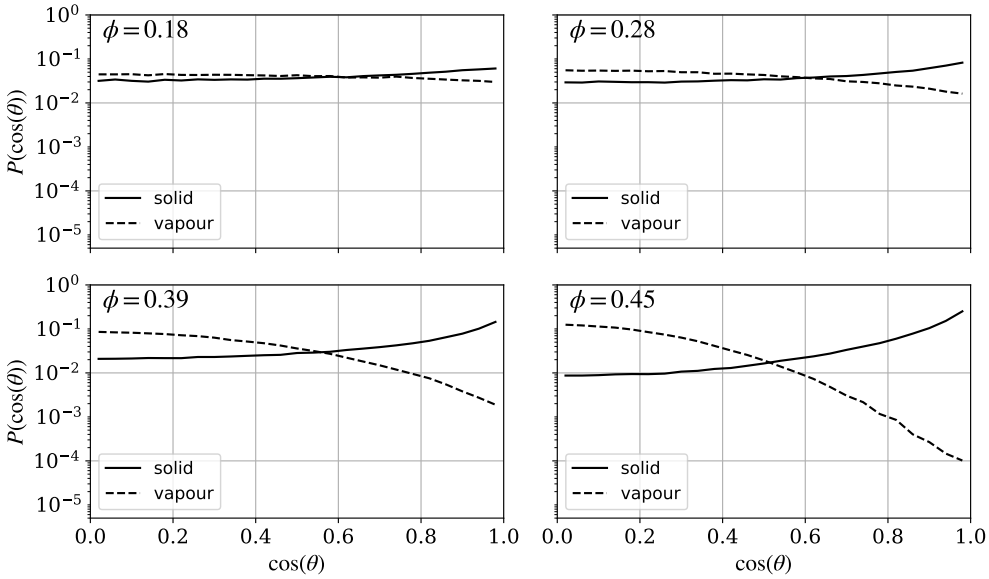

(d) $\kappa = 0.45$

Fig. S6 Orientation distributions at the interfaces in simulations of purely repulsive particles. Solid lines are the distributions at the solid interface and dashed lines are those at the vapour interface.

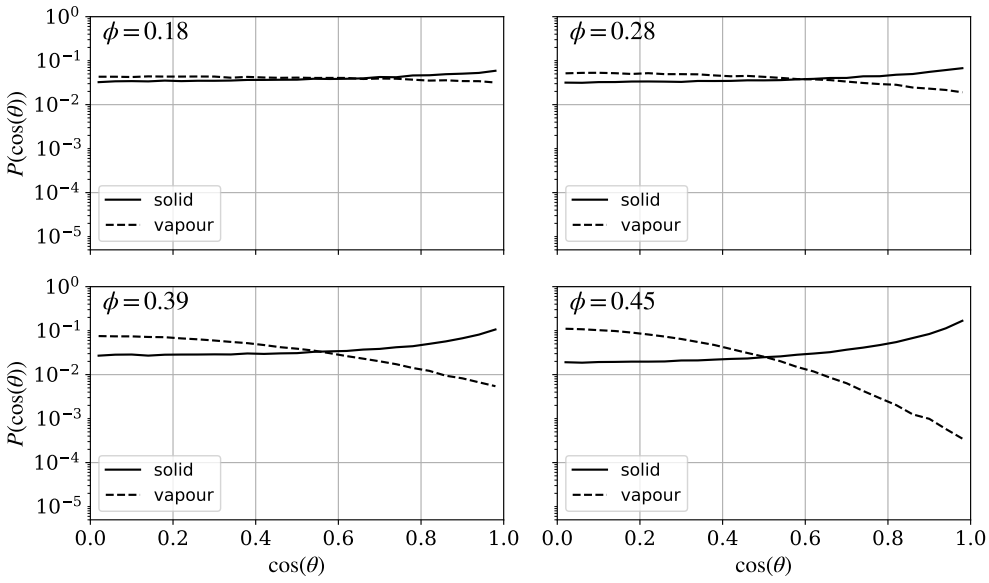

(e) $\kappa = 0.50$

Fig. S6 Orientation distributions at the interfaces in simulations of purely repulsive particles. Solid lines are the distributions at the solid interface and dashed lines are those at the vapour interface.

S7 Packing of close-packed ellipsoids in face-on and side-on orientations

In order to calculate the interaction energy difference between a fluid particle in the face-on or side-on orientation and its nearest neighbours (main paper, eqn (7)), the packing of a layer of fully face-on or fully side-on particles was assumed. Through examination of simulated systems that formed highly aligned layers at either interface (in these cases, the alignment continued into the bulk), it was found that the fluid particles pack in such a way that a face-on particle has six nearest neighbours in the same layer, all in the side–side orientation, while a side-on particle has four nearest neighbours (two face–face, two side–side) in the same layer. It should be noted that the side-on case was somewhat more disordered.

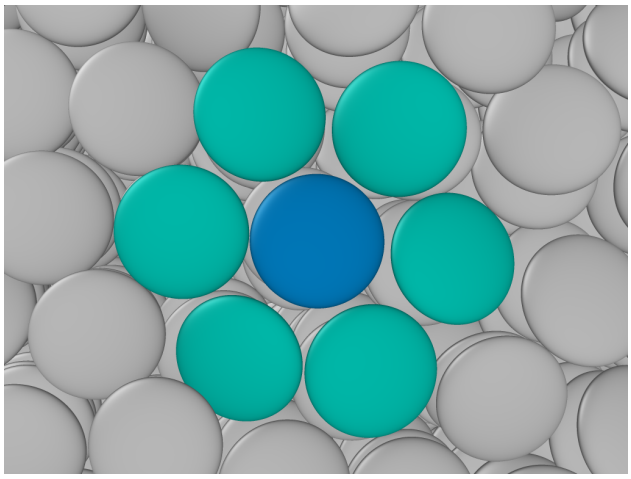

(a) A face-on particle (blue) has 6 nearest neighbours (green) in its closest packing. All six interact in the side–side orientation.

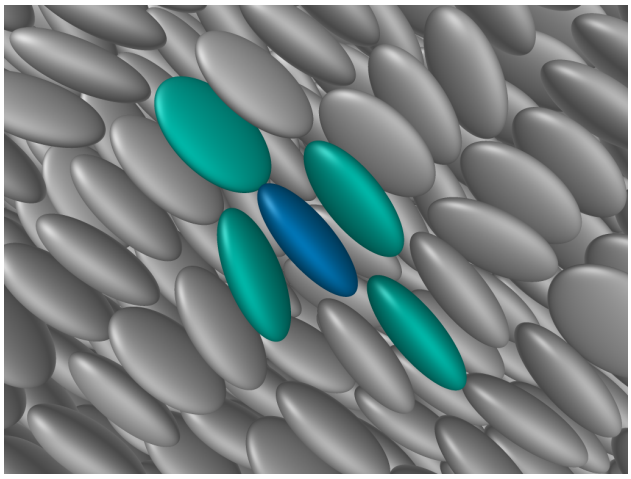

(b) A side-on particle (blue) has four nearest neighbours (green) in the observed packing. Two interact in the face–face and two in the side–side orientations.

Fig. S7 Closest packing of fluid particles in the (a) face-on and (b) side-on orientations to an interface.

Comparing this ideal alignment with systems in which the bulk fluid is isotropic, some deviation from this assumed behaviour is observed, with a more disordered interface in these cases, especially for the side-on orientation at the vapour interface.

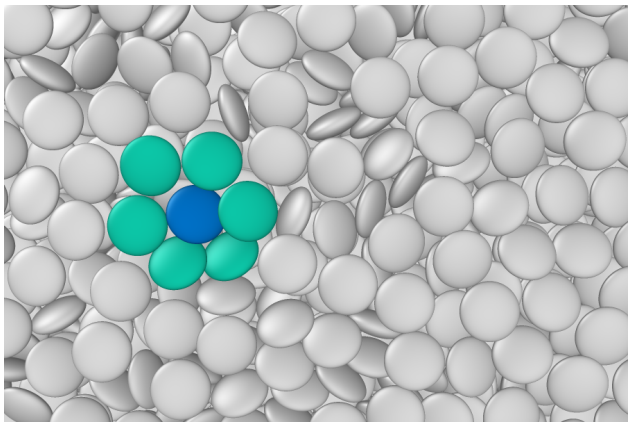

(a) An example of face-on packing at the solid interface in a system in which the bulk fluid is isotropic. Highlighted particles show the assumed packing from Fig. S7(a) for face-on particles.

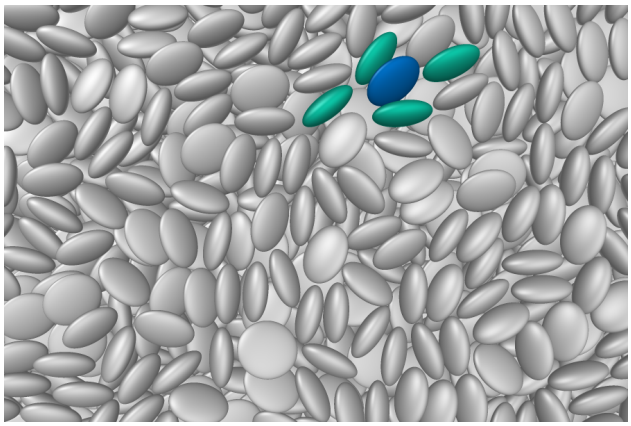

(b) An example of side-on packing at the vapour interface in a system in which the bulk fluid is isotropic. Highlighted particles show the assumed packing from Fig. S7(b) for side-on particles.

Fig. S8 An example of the actual arrangement of particles in (a) the face-on orientation at the solid substrate, and (b) the side-on orientation at the vapour interface. These snapshots come from the system with the strongest alignment at both interfaces (graphene substrate, $\kappa = 0.4$, $\kappa' = 0.3$, $T^* = 0.73$, $\phi_{\mathrm{av}} = 0.49$). Although some instances of the assumed packing are observed at both interfaces, the particles are generally more disordered, especially in the side-on orientation at the vapour interface.

S8 Effect of pressure

In order to maintain a constant, and experimentally relevant (for OSCs), density over the range of parameters and temperatures studied, and to prevent evaporation, the positions of the two walls (repulsive harmonic wall at the vapour interface, and solid wall) were fixed. This resulted in high pressures in some circumstances, with the particles at the vapour interface pushed up against the harmonic wall. Although it does not appear that the pressure influences the orientation at the solid interface significantly (Fig. S9a), there is a slight dependence of the orientation at the vapour interface on pressure (Fig. S9b).

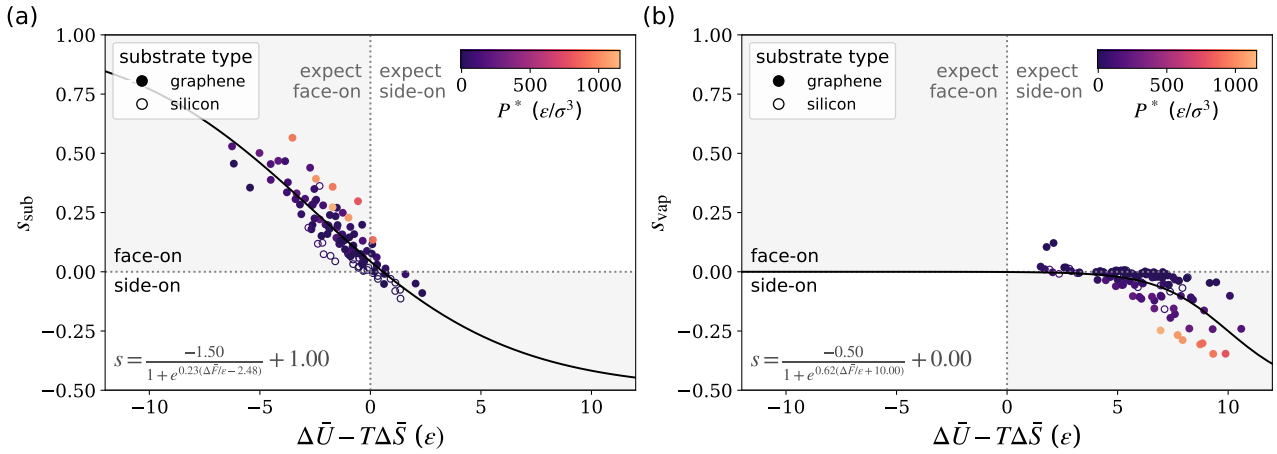

Fig. S9 Orientational order parameter at the (a) solid and (b) vapour interfaces as a function of the interface free energy difference, with points colour-coded by the average reduced pressure ($P^* = P/(\epsilon/\sigma^3)$, calculated from the normal force per unit area on the solid substrate). The scaling of the orientation with free energy difference is largely independent of pressure, except at very high pressures.

References

[1] S. J. Plimpton, *J. Comput. Phys.*, 1995, **117**, 1–19.

[2] W. M. Brown, M. K. Petersen, S. J. Plimpton and G. S. Grest, *J. Chem. Phys.*, 2009, **130**, 044901.

[3] J. G. Gay and B. J. Berne, *J. Chem. Phys.*, 1981, **74**, 3316–3319.

[4] R. Berardi, C. Fava and C. Zannoni, *Chem. Phys. Lett.*, 1998, **297**, 8–14.

[5] R. Everaers and M. R. Ejtehadi, *Phys. Rev. E*, 2003, **67**, 041710.

[6] W. L. Jorgensen, D. S. Maxwell and J. Tirado-Rives, *J. Am. Chem. Soc.*, 1996, **118**, 11225–11236.

[7] C. Lorenz, E. Webb, M. Stevens, M. Chandross and G. Grest, *Tribol. Lett.*, 2005, **19**, 93–98.

[8] P. Becker, P. Scyfried and H. Siegert, *Z. Phys. B Condens. Matter*, 1982, **48**, 17–21.